SUPPLEMENTARY INFORMATION

Selective Recovery of Fascicular Activity in Peripheral Nerves

Brian Wodlinger, Dominique M. Durand

Neural Engineering Center, Department of Biomedical Engineering, Case Western Reserve University, Cleveland OH, 44106 USA

Address correspondence to: D. M. Durand (dxd6@case.edu)

Supplementary Results

Source Localization

Compound action potentials (CAPs) were elicited on the Tibial and Peroneal branches of the Sciatic nerve in Rabbit, as described in the methods. The Transformation matrix was applied to the peak of these CAPs, resulting in an estimate of the location of the activity within the nerve cross-section for each source. Figure S1 presents these estimates overlayed onto nerve histology from each experiment in a diagram of the cuff. The signals overlay the approximate location of each fascicle group. Histological sections of the branches were used to verify that, in every case, the fascicles covered by the estimate were part of the branch stimulated.

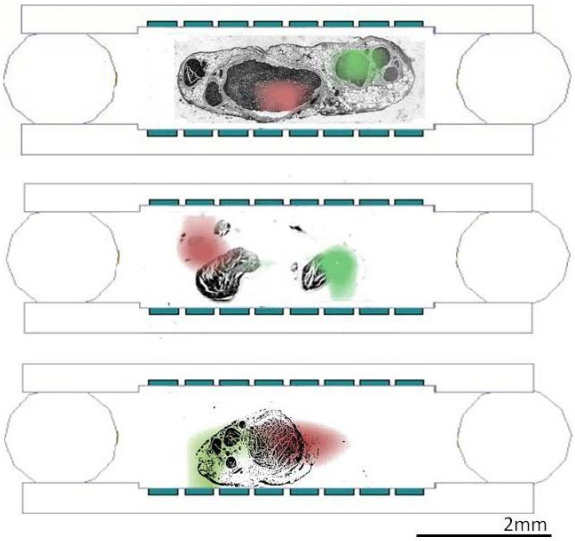

Figure S1: Localization of Sources. These images show the locations estimated using the beamforming algorithm, with nerve histology overlayed and a schematic of the cuff, for reference. The tibial branch signals are in red, while peroneal branch signals are in green – in every case they overlap the correct group of fascicles. Note that the position of the nerve histology within the cuff is approximate.

Synchronous Evoked Activity

130Hz sinusoidal stimulation applied to each fascicle was found to elicit CAP-like discharges from the nerve superimposed on the artifact (Figure S2A). Since the artifact was sinusoidal, it could easily be removed using notch or high-pass filters by a minimum of 100dB as shown in Figure S2B. These signals increased in amplitude and complexity with increasing stimulation amplitude and had a signal to noise ratio of 22±5 dB calculated using the peak-to-peak amplitudes of the signal and noise. When this same stimulation is applied after the nerve has been ligated or severed, no signal above noise baseline is recorded. Similarly, this activity is observed long after the associated muscles have fatigued, confirming its neural origin.

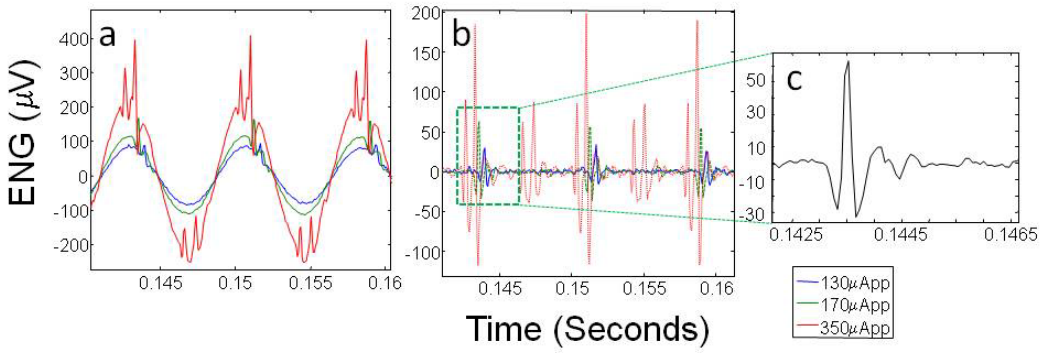

Figure S2: 130Hz Sinusoidal stimulation produces CAP-like neural responses with variable amplitude, delay, and complexity as the stimulation intensity is raised. (A) Recording high-pass filtered at 100Hz, (B) the same signal high-pass filtered at 800Hz. (C) A sample spike from the 170μApp stimulation level. Note that the filter has effectively removed all traces of the stimulus artifact (119dB rejection).

Effect of Contact Density and Position on Signal Recovery

In order to determine the role of contact density the above experiments were repeated with 8 instead of 16 contacts and with other recording configurations produced by removing rows from the transformation matrix and recorded data. Two different configurations were tested: 1) top half of the electrode only, and 2) evenly numbered contacts only. The transformation matrix was recalculated using equations 1 and 2 with the appropriate rows of the lead-field matrix removed; the Tibial and Peroneal filters were then recalculated using the SBF algorithm. The correlation coefficient was calculated between the output of these reduced tibial or peroneal filters on the mixed-branch signal and the full tibial or peroneal filter (ie, all 16 channels active) operating on the single branch signal to determine the relative quality of the techniques. The results indicate that any decrease in the contact density produced a significant decrease in the cross-correlation coefficients.

For the 7 nerves implanted, with 2 sources for each nerve, reducing the number of contacts to 8 from the full 16 contacts (2/mm) decreased R^2 value by 0.34±0.27, from 0.81±0.08 to 0.47±0.28 when only the top half of the electrode is used and by 0.22±0.18 to 0.59±0.19 when only the evenly numbered contacts are used. The best single-channel recordings (best channel chosen

based on the highest R^2 value), showed a significant reduction in accuracy compared to the full 16-channel SBF algorithm, however this reduction is lost when the number of contacts is reduced, suggesting a certain contact density is required to achieve the full benefits of the algorithm. A full comparison of all of the different test configurations is available in Table 1, for all values n=14 and single-sided paired t-tests were used to determine statistical significance. Data was tested for normality with the Anderson-Darling test.

TABLE I

SUMMARY OF LARGE SIGNAL RECOVERY ACCURACY

Test Case	Filter Calculation	Number of Contacts	Configuration of Contacts	R^2	Reduction in Performance	Statistical Significance
Source based filters (SBF)	Source-based	16	Full	0.81±0.08	0	
Single pixel filter	Single row of Transformation Matrix	16	Full	0.64±0.14	0.18±0.09	p<0.0002
Even Electrode	Source-based	8	Even Numbered Only	0.59±0.19	0.22±0.18	p<0.0003
Half Electrode	Source-based	8	Top Half Only	0.47±0.28	0.34±0.27	p<0.000075
Best *a posteriori* Channels	None	16	Full	0.58±0.14	0.24±0.11	p<0.000006
Best *a posteriori* Channels	None	8	Even Numbered Only	0.56±0.14	0.26±0.10	p<0.0000009
Best *a posteriori* Channels	None	8	Top Half Only	0.53±0.19	0.29±0.18	p<0.00002

Pseudo-Random Neural Activity

The previous section investigated the accuracy of the algorithm acting directly on the high amplitude, short-burst neural activity such as generated during movements such as reflex activity. However, most neural activity in peripheral nerves is desynchronized. Desynchronized, pseudo-spontaneous activity with controlled timing and amplitude was elicited using 5 or 10kHz sinusoidal stimulation. Since axonal refractory periods are longer than a single period of this stimulation, axons are unable to fire synchronously and the activity becomes pseudorandom[4]. The recorded signals were digitally filtered between 800-3000Hz to remove any artifact or EMG contamination.

These signals have similar amplitude, power spectra, and statistical distribution to spontaneous nerve activity. Since they can be precisely controlled in both time and amplitude by stimulation, they provide a repeatable and versatile method to generate realistic neural activity artificially. Figure S3 compares this pseudo-spontaneous evoked activity with activity recorded during voluntary inspiration from a cuff electrode chronically implanted on a canine hypoglossal nerve[1, 5]. Part A shows an example of ENG recorded during a voluntary inspiration from the hypoglossal nerve in chronic dog preparation, while part B shows signals with similar shape recorded during four separate 5kHz trials at four different amplitudes after artifact removal. Figure S3c compares the power spectra of these recordings (here filtered with a wider 100Hz-4kHz band for comparison) with each other and the voluntary recording of part A. The spectra have similar peaks, although the canine recording appears to have a higher proportion of high frequency power, potentially due to the mixture of fibers in the nerve, or the effect of encapsulation. The range of amplitudes evoked is shown in part D, along with the variance in RMS value calculated using 1 second bins. These values range from less than 2 μV_{rms} to more than 12μV_{rms}. This is comparable to values of 2-5 μV_{rms} reported during chronic inspiration and acute sensory recordings[1, 6], although larger values such as those achieved here may be expected due to the stronger motor fibers present in this nerve. As above, when this stimulation is applied after the nerve has been ligated or cut, the recorded signal shows no increase in power over baseline noise level, confirming the neural origin of the signal.

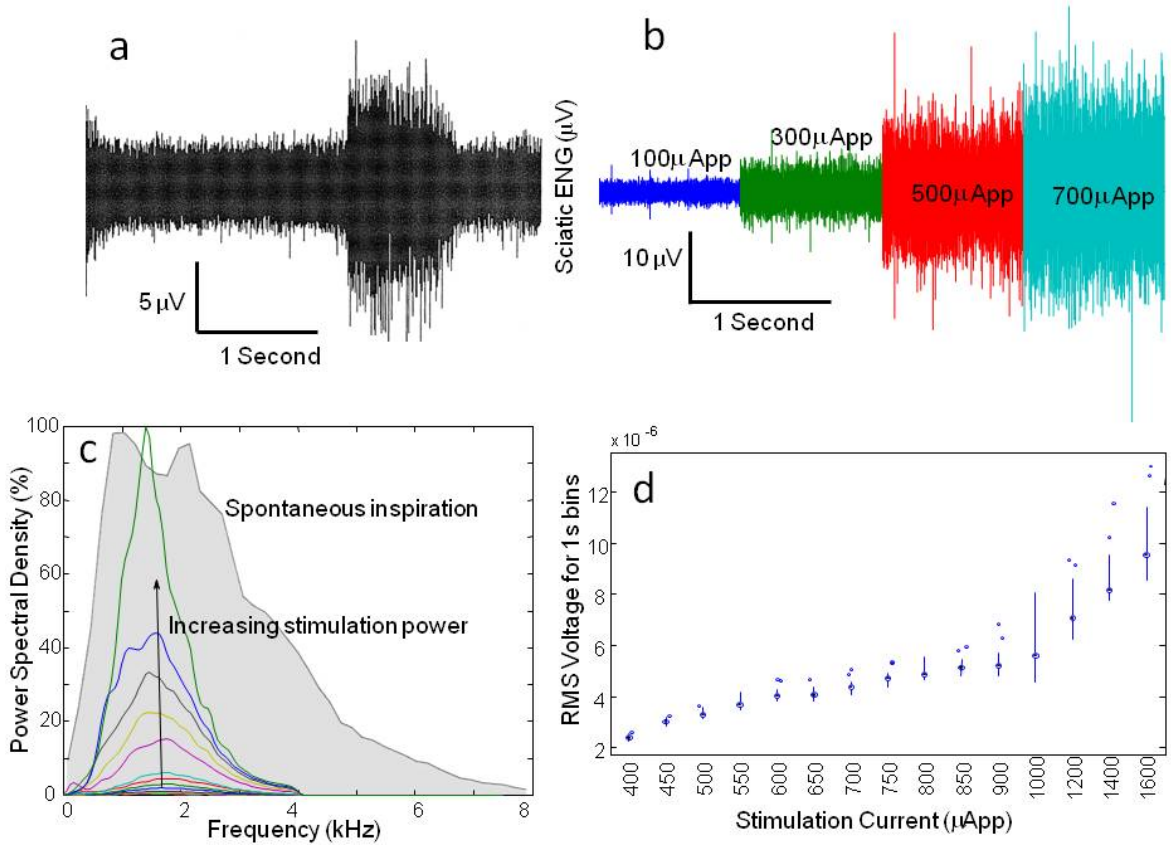

Figure S3: Generating Pseudo-spontaneous activity. (A) ENG recorded chronically on the hypoglossal nerve of a canine[1] during spontaneous inspiration, shown here for comparison with the 5kHz evoked neural signals recorded during these experiments. (B) ENG signals during 5 KHz stimulation of the tibial branch, filtered 800-3000Hz at four different intensities. Each intensity was recorded during a separate but sequential trial and a segment from each is shown side-by-side here for comparison. The power of the signal increases as the stimulation intensity (denoted by or on each segment) increases. (C) Comparison of power spectral density (Welch's method) for various levels of 5kHz stimulation with signal in A. (D) Box and whisker plot of power in recorded signal for each stimulation intensity applied. Points above each column represent outliers. The stimulation artifact has been effectively rejected to more than 40dB below signal level in all cases.

Classification

To determine the ability of the algorithm to recover lower SNR signals that have properties similar to motor activity within the nerve, pseudo-spontaneous activity was generated by stimulating one of the two branches individually with 5 or 10 kHz sinusoids (Figure S3). 30-second 16-channel ENG data sets were recorded on the main sciatic trunk, and divided into 100ms bins. One recording was made for each stimulation intensity on each branch of 6 sciatic nerves. The root-mean-square (RMS) power was calculated for each bin on each of the 16 channels. The beamforming filters for the tibial and peroneal branches were then applied giving an estimate for the activity level in each branch. The larger of the two estimates was used to

predict which branch had been stimulated. The accuracy over six experiments is plotted against the stimulation level in Figure S4.

Pseudo-spontaneous signals were able to generate muscle contraction and the threshold amplitude required to generate motor activity was measured (Mth). The amplitude was then varied between <50% of MTh, to >300% as in Figure S4. For very low stimulation levels (<50% of MTh) the classification accuracy is approximately at chance level, however as the stimulation increases, the resulting neural signal also increases saturating at approximately 150% of MTh, after which the mean is relatively constant while the standard deviation shrinks. Over 150% of the motor threshold, the classification accuracy is 98±4%. Muscle fatigue was not observed to have a noticeable effect on the recorded signals or classification accuracy.

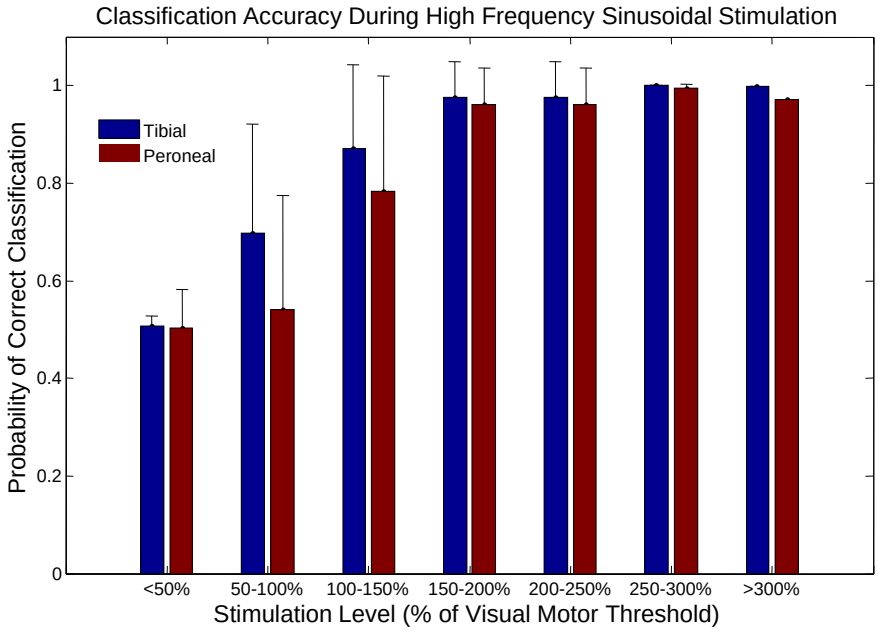

Figure S4: Classification Accuracy for a simple 2-class system of Tibial or Peroneal activity during 5 or 10kHz stimulation. Data were broken down into 100ms bins in order to take the RMS and apply the beamforming filters. The Tibial filter value with the Peroneal filter value were compared for each bin and the higher of the two estimated as the active branch. Above 150% of muscle threshold, the algorithm identified the correct branch in more than 98±4% of the 100ms windows.

Amplitude Dependence of the Recovered Signals

In order to determine the ability of the algorithm to recover proportional control signals, the outputs of the Tibial and Peroneal filters were analyzed over various stimulation amplitudes. The results are plotted in Figure S5 for a typical experiment. 5kHz stimulation was applied for 30 seconds at a variety of intensities to the tibial branch only. The recorded signals were split into 1s bins, and the RMS power on each channel, in each bin was calculated. The Tibial and Peroneal filters were the applied to obtain the activity level of each source during each bin. The

results indicate that the estimated power in the stimulated source (blue) was significantly higher than the estimated power in the unstimulated source (red) at all the amplitudes of stimulation tested. The separation between the responses for each level of stimulation suggests that it is possible to distinguish multiple levels of activity, rather than simpler all-or-nothing binary classification. In order to evaluate the information transfer in these data, a linear discriminant analysis classifier was trained with 10% of the data from each experiment and tested on the remaining 90%. The classifier was used to predict which stimulation intensity (class) a given 100ms bin's power level belonged to, and calculate the resulting accuracy over the range of intensities tested. This accuracy was used with Equation 6 to calculate the bit-rate or throughput. The results show that for six experiments the total bit transfer rate was 8±4 bps for each 2-source nerve.

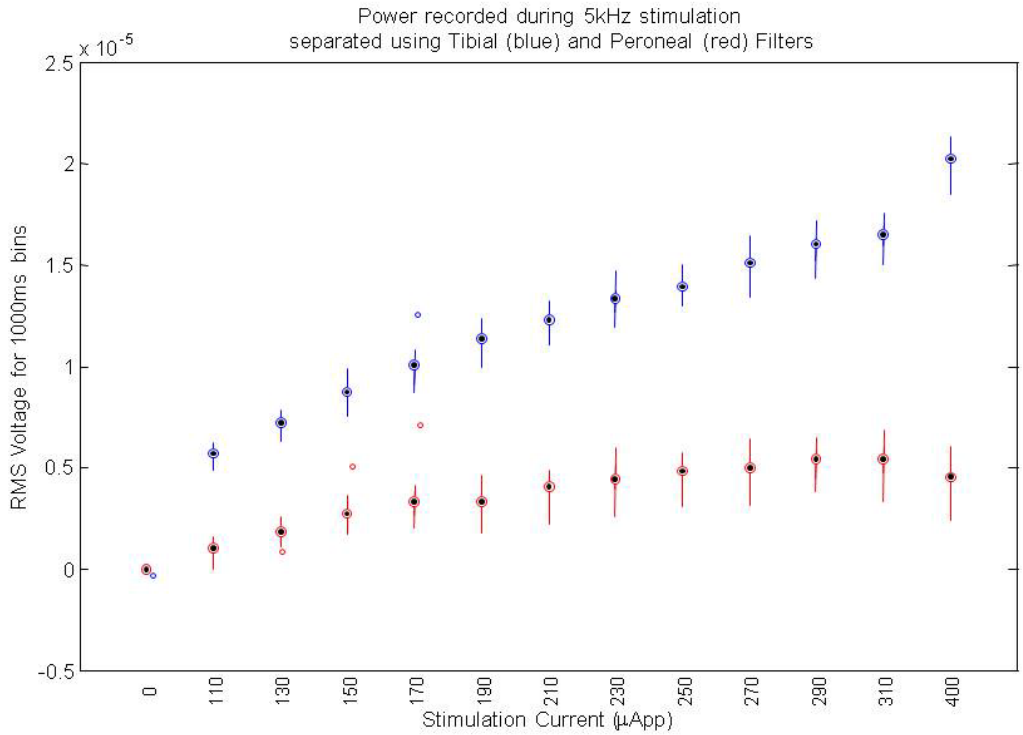

Figure S5: Box plot of the outputs of the Tibial and Peroneal filters acting on binned RMS data during Tibial (blue) stimulation. Note that the blue values show a higher mean, and a much clearer trend with increasing stimulation intensity. In order to take into account resting activity levels, an offset was applied to each filter output to force their mean to be zero at zero stimulation current. Long (1sec) bins were used to show the trend clearly.

Convergence of the Source-Based Filters

Convergence of the iterative SBF algorithm presented here was monotonic for all experimental data. In all cases successive iterations provided steadily decreasing improvements to the signal to interference ratio, and in all cases at least some improvement was observed. Poor convergence seemed to coincide with the fascicular sources being closer together, and so more

difficult to separate (as judged by the estimated localization and the raw spatial signal). The number of cycles required to reach threshold depended strongly on the rate of convergence used.

Application to a Simulated Human Case

In order to examine the quality of control signals that might be expected in a more complex case, a finite element model of the human femoral nerve with 10 active fascicles split into 5 groups based on muscle innervated was used. A full description of this model is available in Wodlinger and Durand[3]. Independent signals were generated for each of the 5 groups using Poisson-distributed action potentials with a time-varying lambda value. These action potentials were distributed over axons in each of the fascicles of the group, over a range of axon diameters. The signals were then summed, and Gaussian noise added with the same variance as the signal (i.e. SNR=1). Using the SBF algorithm, these signals were separated and the correlation coefficients between the recovered mixed-signals and the recovered single-group inputs calculated. Figure S6 shows an example trial where 3 of the 5 signals are recovered well (R^2>0.7), and one other (E) may still be suitable for binary control, if not proportional. The mean R^2 value in these tests was 0.7. The source based filters for this test were calculated based a separate 100ms segment of single-group activity for each group at the same noise level, as might be provided in an amputee through attempted training movements.

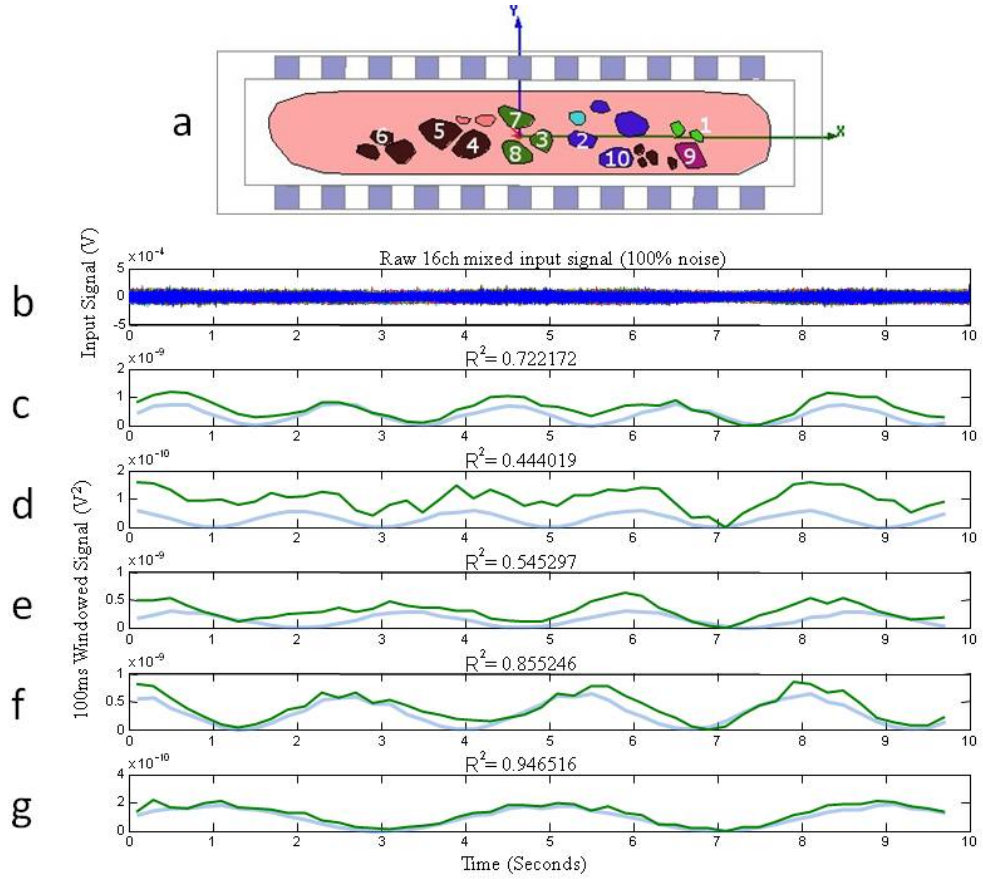

Figure S6: Simulated Signal Recovery in a Human Nerve. A) Finite Element Model of human sciatic nerve[2], showing the 10 fascicles selected for this experiment color-coded with the muscle group innervated. B) Raw 16ch input signal containing mixed activity from 5 independent fascicular groups. C-G) Recovered mixed-signal activity for each fascicular group (thin green line) compared with the recovered single-group input signal (thick blue line). Both signals are RMS averaged in 100ms bins for noise rejection. Fascicles are grouped as in Table III of Wodlinger and Durand[3], representing the rectus femoris, vastus lateralis and medialis, saphenous and sartorius muscles.

References

[1] M. Sahin, "Chronic Recordings of Hypoglossal Nerve in a Dog Model of Upper Airway Obstruction," Cleveland: Case Western Reserve University, 1998.

[2] M. A. Schiefer, R. J. Triolo, and D. J. Tyler, "A model of selective activation of the femoral nerve with a flat interface nerve electrode for a lower extremity neuroprosthesis," *IEEE Trans Neural Syst Rehabil Eng*, vol. 16, pp. 195-204, Apr 2008.

[3] B. Wodlinger and D. M. Durand, "Localization and Recovery of Peripheral Neural Sources With Beamforming Algorithms," *Ieee Transactions on Neural Systems and Rehabilitation Engineering*, vol. 17, pp. 461-468, Oct 2009.

[4] J. T. Rubinstein, B. S. Wilson, C. C. Finley, and P. J. Abbas, "Pseudospontaneous activity: stochastic independence of auditory nerve fibers with electrical stimulation," *Hear Res*, vol. 127, pp. 108-18, Jan 1999.

[5] M. Sahin, M. A. Haxhiu, D. M. Durand, and I. A. Dreshaj, "Spiral nerve cuff electrode for recordings of respiratory output," *J Appl Physiol*, vol. 83, pp. 317-22, Jul 1997.
[6] S. Micera, W. Jensen, F. Sepulveda, R. R. Riso, and T. Sinkjaer, "Neuro-fuzzy extraction of angular information from muscle afferents for ankle control during standing in paraplegic subjects: an animal model," *IEEE Trans Biomed Eng*, vol. 48, pp. 787-94, Jul 2001.